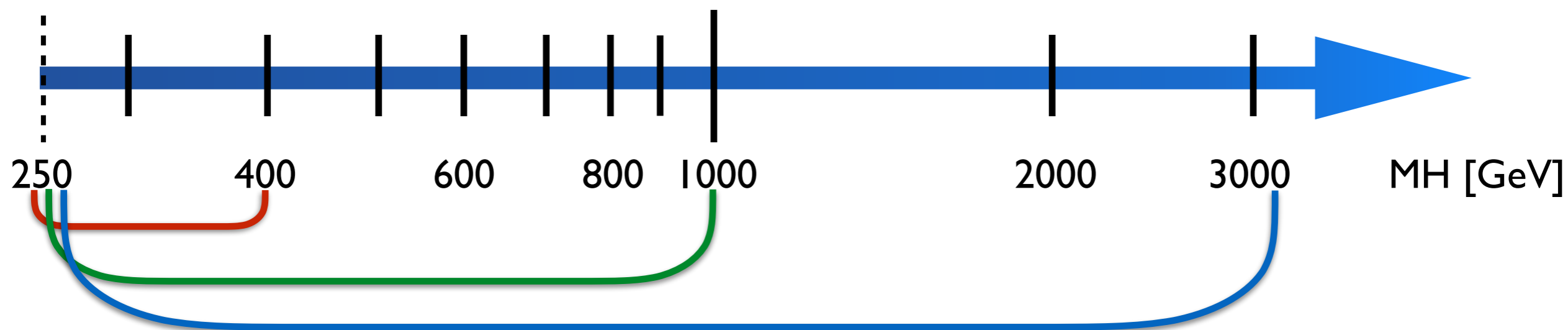


Searches for double Higgs production or decay using the CMS detector

Giacomo Ortona¹, for the CMS collaboration

1. Introduction
2. Double Higgs searches in CMS:
 - A. $bb\gamma\gamma$
 - B. $bbbb$
 - C. $bbWW$
 - D. $bb\tau\tau$
3. Results and Conclusions

Motivations: Resonant searches



MSSM/2HDM: Additional Higgs doublet \rightarrow CP-even scalar H.

- We can probe the low m_A /low $\tan\beta$ region where $BR(H \rightarrow h(125)h(125))$ is sizeable.

Singlet model: Additional Higgs singlet with an extra scalar H.

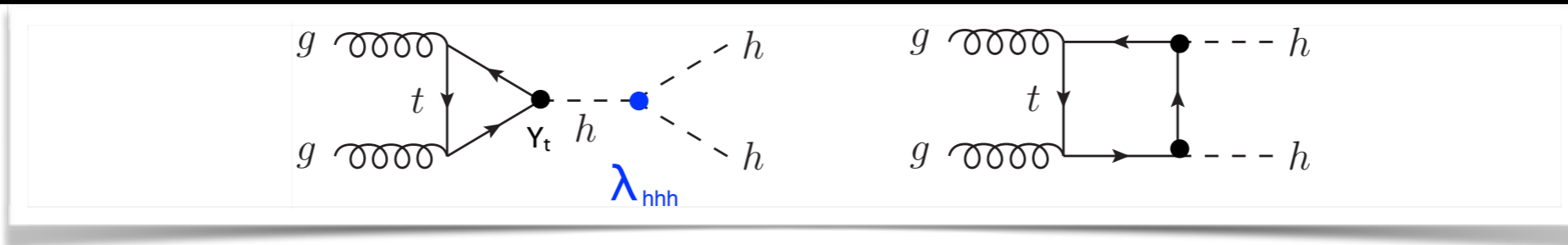
- Sizeable BR beyond $2 \times m_{top}$, non negligible width at high m_H .

Warped Extra Dimensions:

spin-2 (KK-graviton) and spin-0 (radion) resonances.

- Different phenomenology if SM particles are allowed (bulk RS) or not (RSI model) in the extra dimensional bulk

Motivations: Non-resonant searches

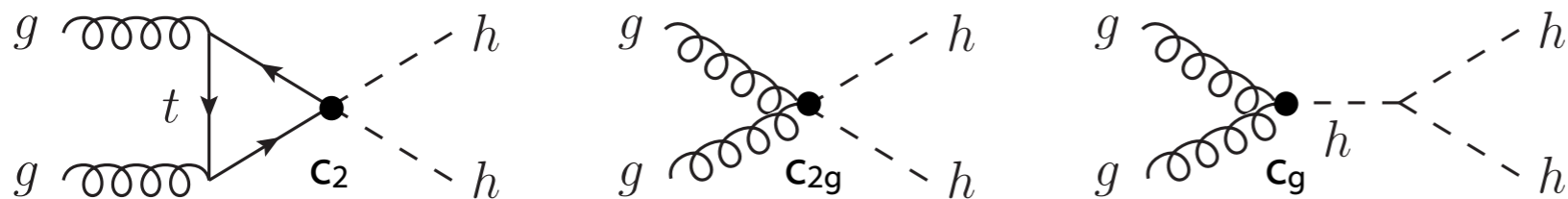


$$\sigma_{hh}^{\text{SM}}(13\text{TeV}) = 33.45\text{fb}^{+4.3\%}_{-6.0\%}(\text{scale unc.}) \pm 3.1\%(\text{PDF} + \alpha_s \text{ unc})^{[1]}$$

The non-resonant double Higgs production allows to directly probe the Higgs trilinear coupling (λ_{hhh}). Even if in Run2 we not have full sensitivity to “measure” SM λ_{hhh}

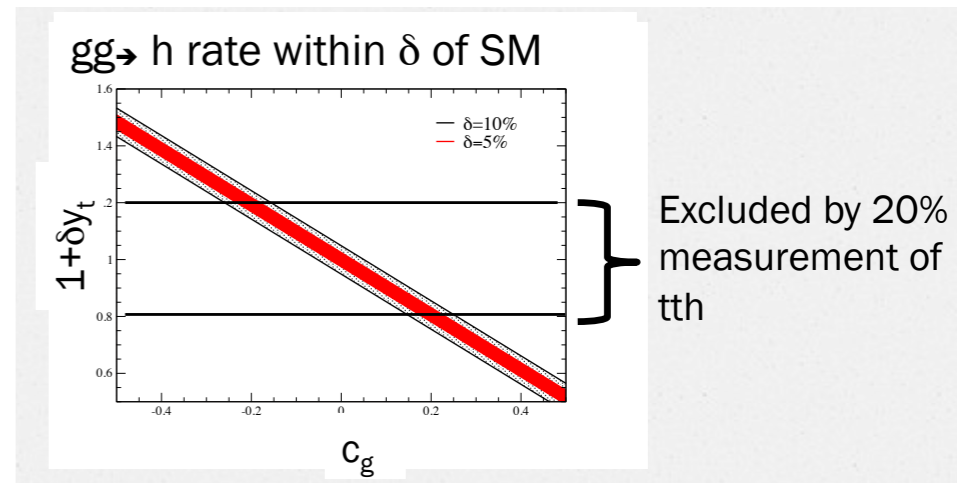
→ The BSM physics can be modelled in EFT adding dim-6 operators^[2] to the SM Lagrangian, and the physics can be described with 5 parameters: λ_{hhh} , γ_t , c_2 , c_{2g} , c_g

- Non SM top Yukawa and λ_{hhh} couplings
- New diagrams and couplings in the game



To be noted :

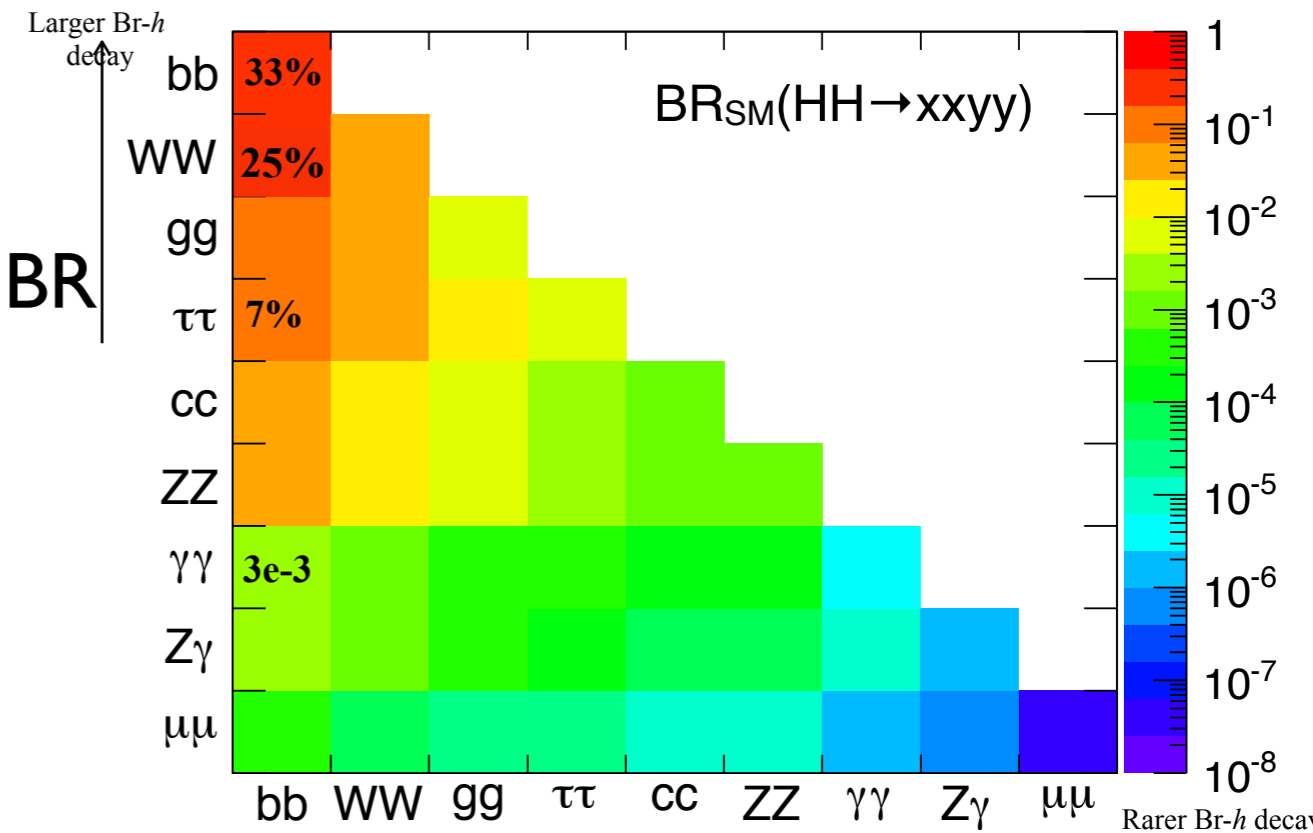
in a linear EFT $c_g = c_{2g}$ and $c_2 = -(3m_t/2v)\gamma_t$



[1] LHCHSWG Yellow Report 4
 [2] Phys. Rev. D91 (2015), no. 11, 115008

CMS searches

- 4 different searches presented today:
 - $bbbb$, $bbWW$, $bb\tau\tau$, $bb\gamma\gamma$
- At least one $h \rightarrow bb$ to have large enough BR
- Rare processes, low σ , complex environment
- Resonant and non-resonant searches performed in Run I and Run 2
- Run I:



- $bbbb$ Resonant: [PLB 749 \(2015\) 560](#), [arXiv:1602.08762](#)
- $bb\tau\tau$ Resonant: [PLB 755 \(2016\) 217](#), [PAS-EXO-15-008](#) Non-resonant [PAS-HIG-15-013](#)
- $bb\gamma\gamma$ Resonant and Non-resonant: [arxiv:1603.06896](#)

Run 2:

- $bbbb$ Resonant: [PAS-HIG-16-002](#), [PAS-B2G-16-008](#)
- ★ $bb\tau\tau$ Resonant: [PAS-HIG-16-029](#), ★ Non-resonant [PAS-HIG-16-028](#)
- $bbWW$ Resonant [PAS-HIG-16-011](#), ★ Non-resonant: [PAS-HIG-16-024](#)

I will focus on the results at $\sqrt{s} = 13\text{TeV}$

Searches: how and where

3 Datasets used for this presentation:

- Run 1, $\sqrt{s}=8$ TeV, $\mathcal{L}=17.9-19.7$ fb⁻¹
- Run 2, 2015, $\sqrt{s}=13$ TeV, $\mathcal{L}=2.3-2.7$ fb⁻¹
- Run 2, 2016, $\sqrt{s}=13$ TeV, $\mathcal{L}=12.9$ fb⁻¹

B-tagging algorithm to identify b-jets from jet constituents

- CSVv2: Based on displaced tracks+secondary vertexes MVA^[1]

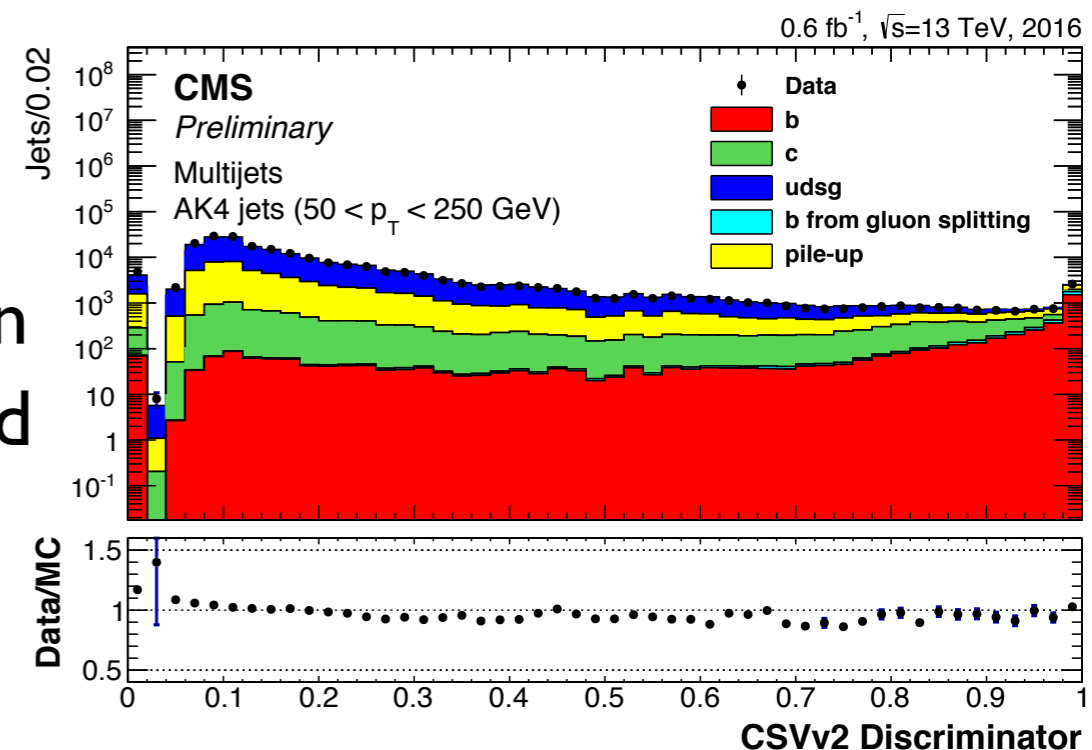
At high $m_H \rightarrow$ boosted regime \rightarrow merged jets

- Reconstruction using substructure information for jets, b-tag
- bbbb, bb $\tau\tau$ channels

Trade-off between BR and contamination, complementarity among channels

- **bbbb**: highest BR, high QCD/ $t\bar{t}$ contamination
- **bbWW**: high BR, large irreducible $t\bar{t}$ background
- **bb $\tau\tau$** : relatively low background and BR
- **bb $\gamma\gamma$** : high purity, very low BR

[1]JINST 8(2013) P04013



hh → bbγγ: run1 results

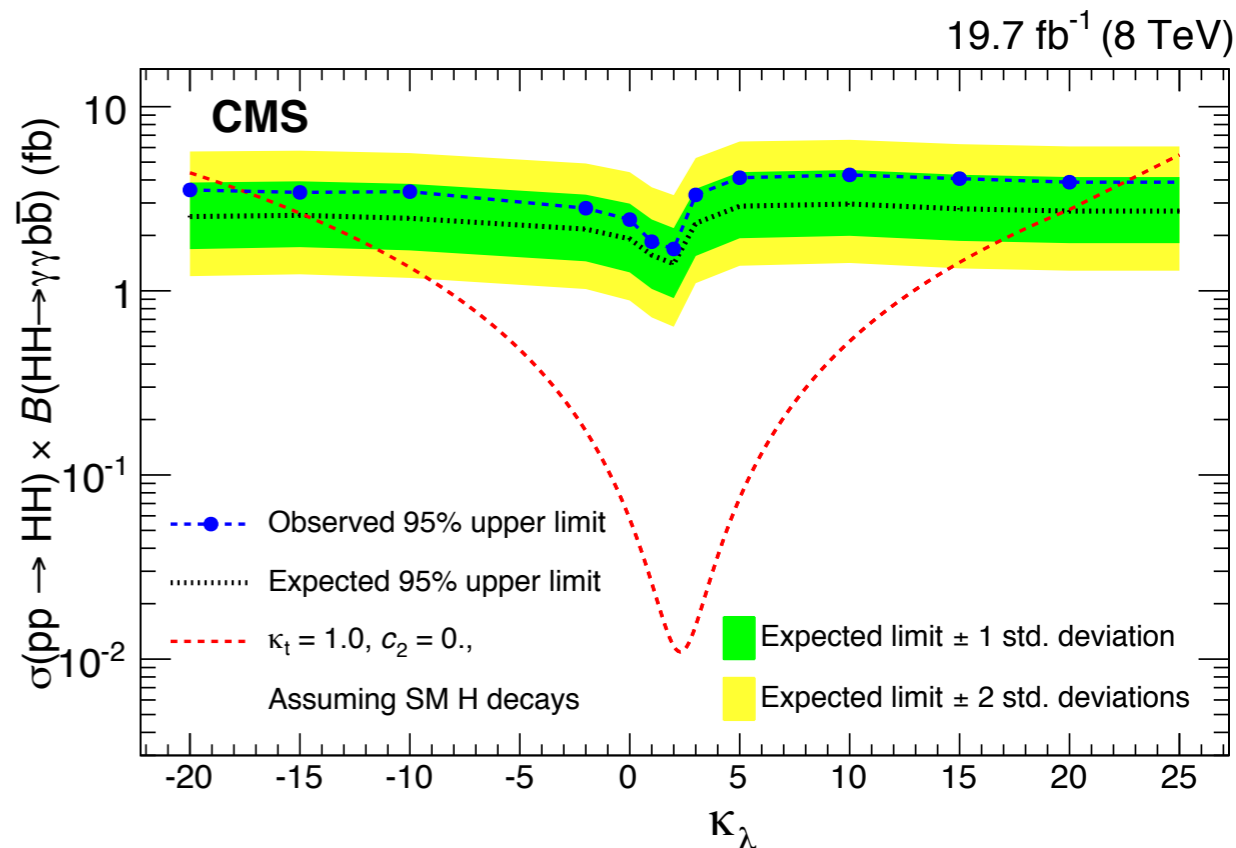
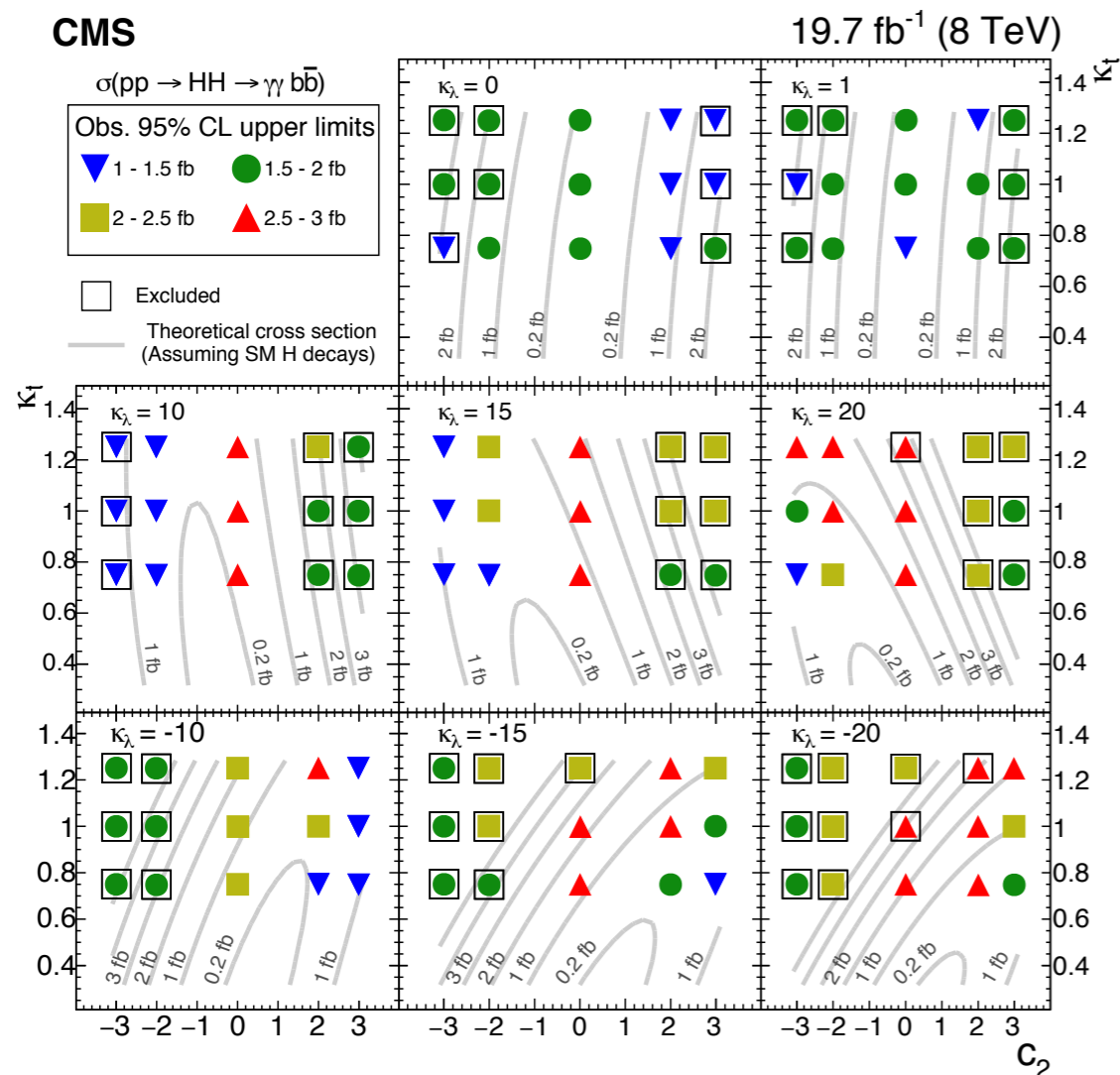
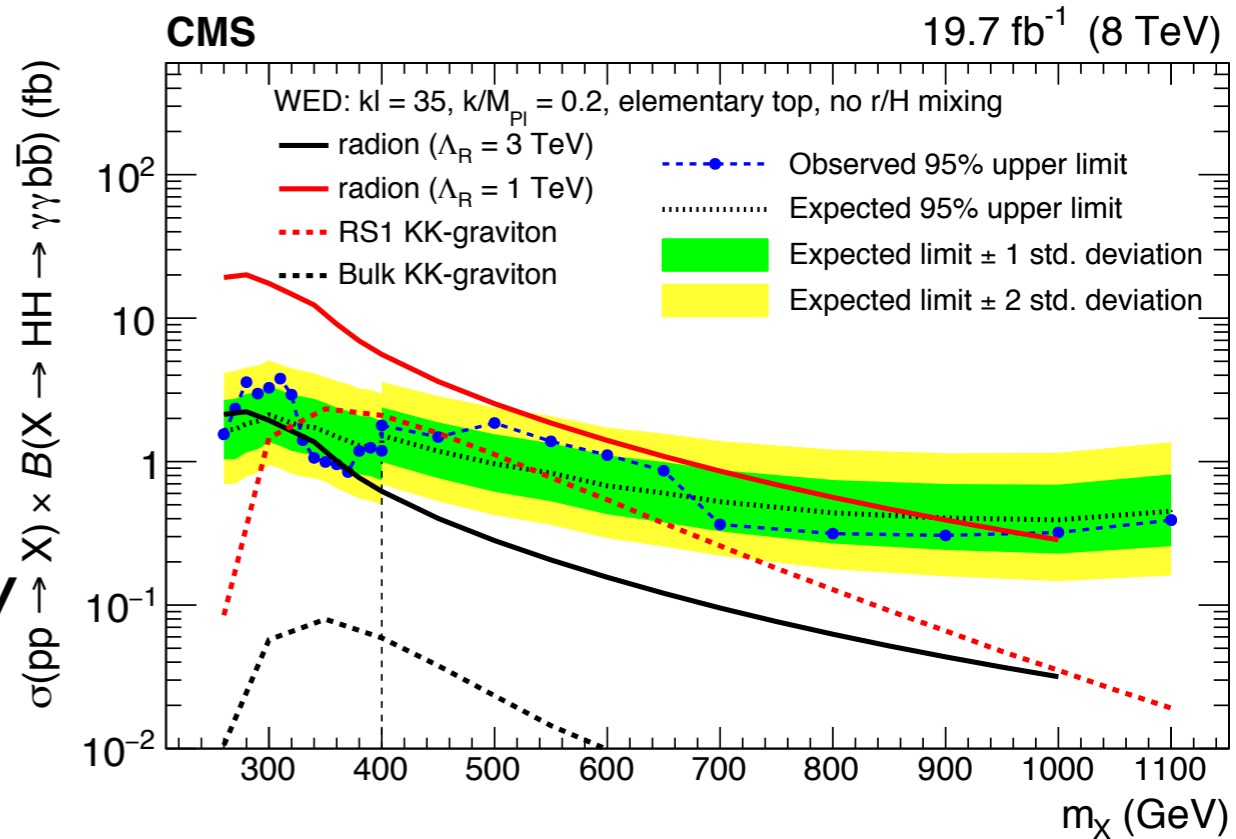


Lowest BR among all channels, but excellent resolution on $m_{\gamma\gamma}$

No excess observed in resonant searches.

Already sensitive to BSM physics below 1 TeV

Non-resonant sensitivity $\sim 70 \times \text{SM}$. Limits in a 3D phase space region $(\kappa_\lambda, \kappa_t, c_2)$ of EFT theory



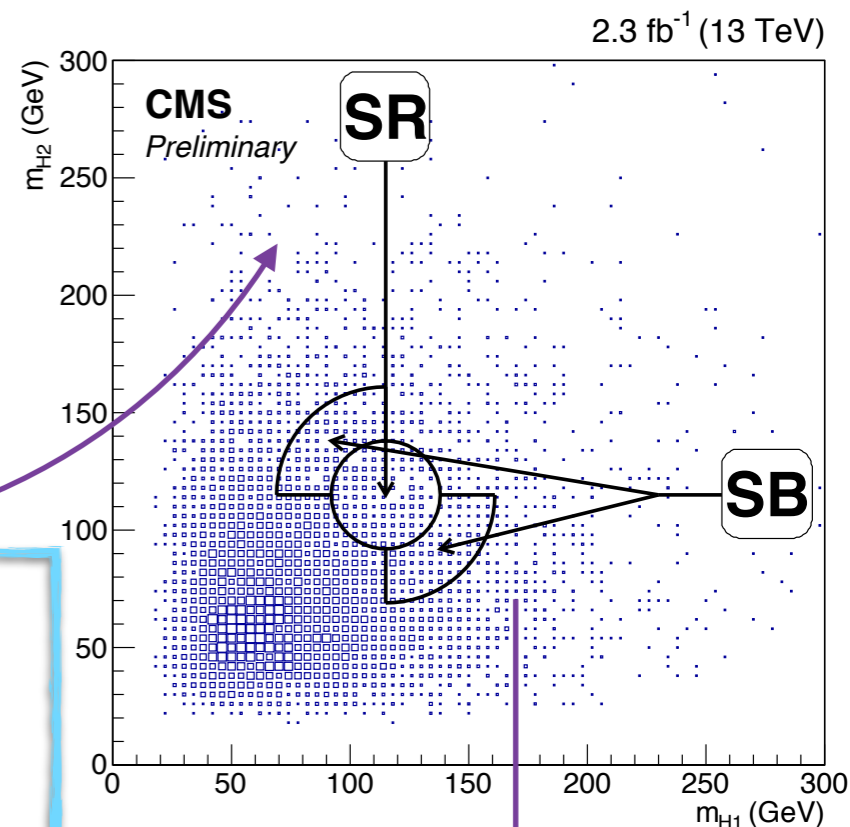
hh → bbbb

Very sensitive channel in the resonant searches

b-tagging at trigger level, ≥ 4 b-jets offline

Low Mass Region ($m_H < 400$) and High Mass Region ($400 < m_H < 1200$) studied separately

Background shape estimation from data in LMR, HMR

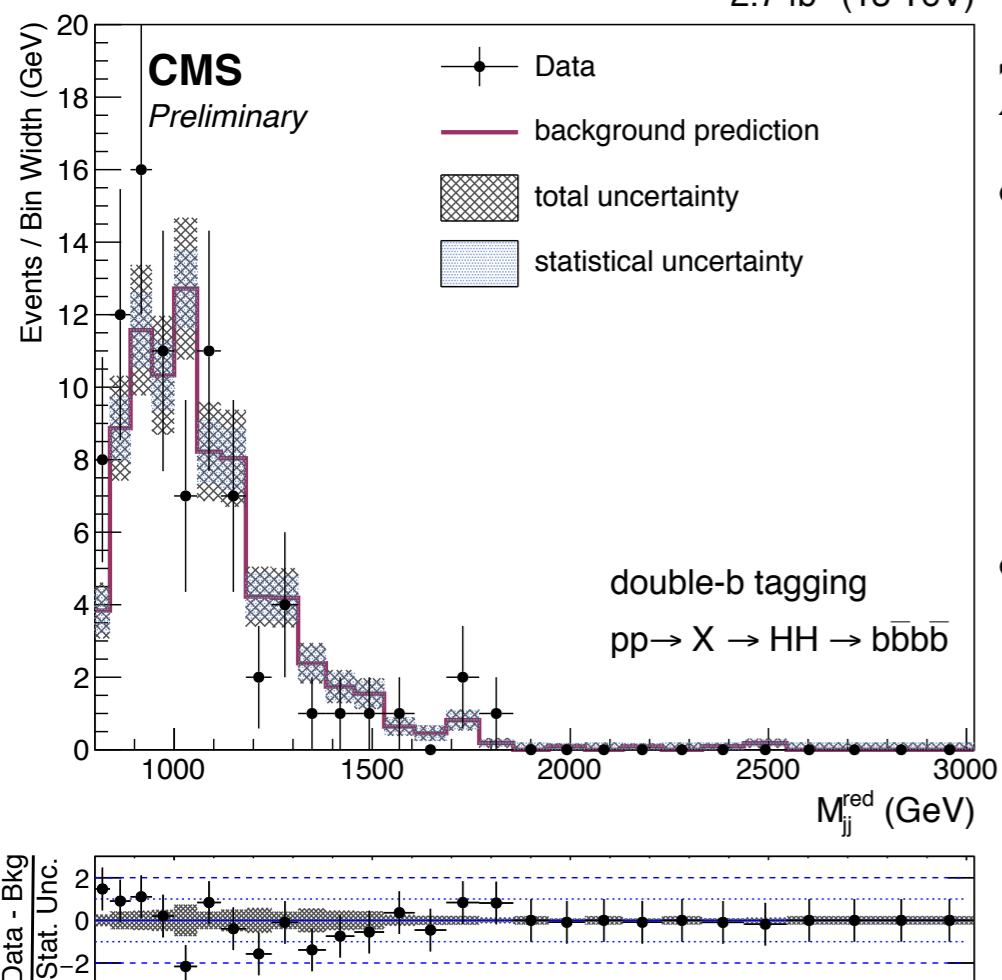
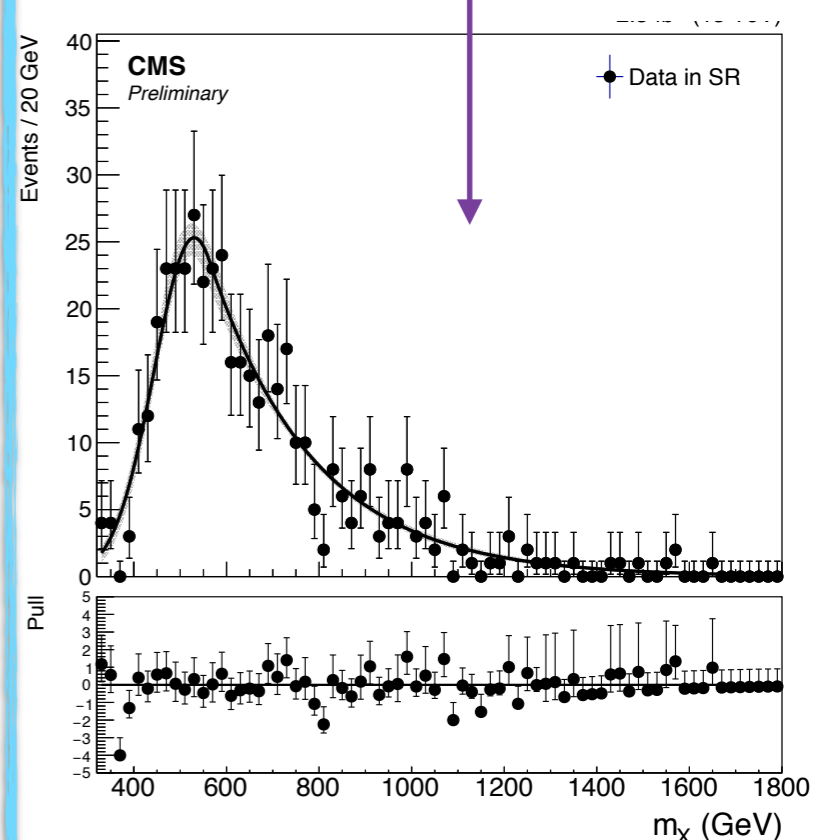


Dedicated **boosted analysis** above $M_H = 1$ TeV

2.7 fb⁻¹ (13 TeV)

2 analysis strategies:

- **double b-tagger**: BDT from jet properties + background estimation from multiple sidebands
- **subjet b-tag**: background fit + 3 categories based on number of b-tagged sub-jets

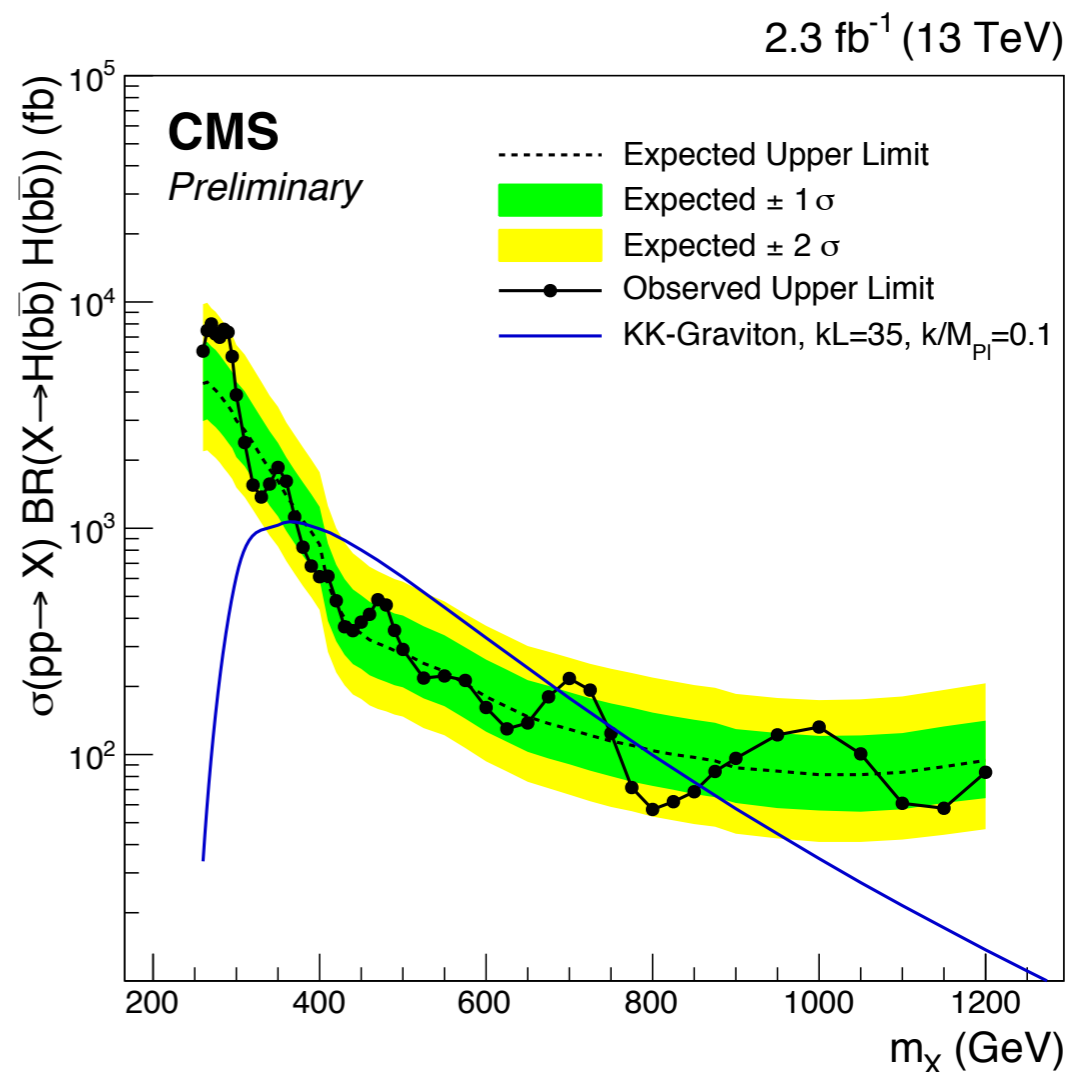
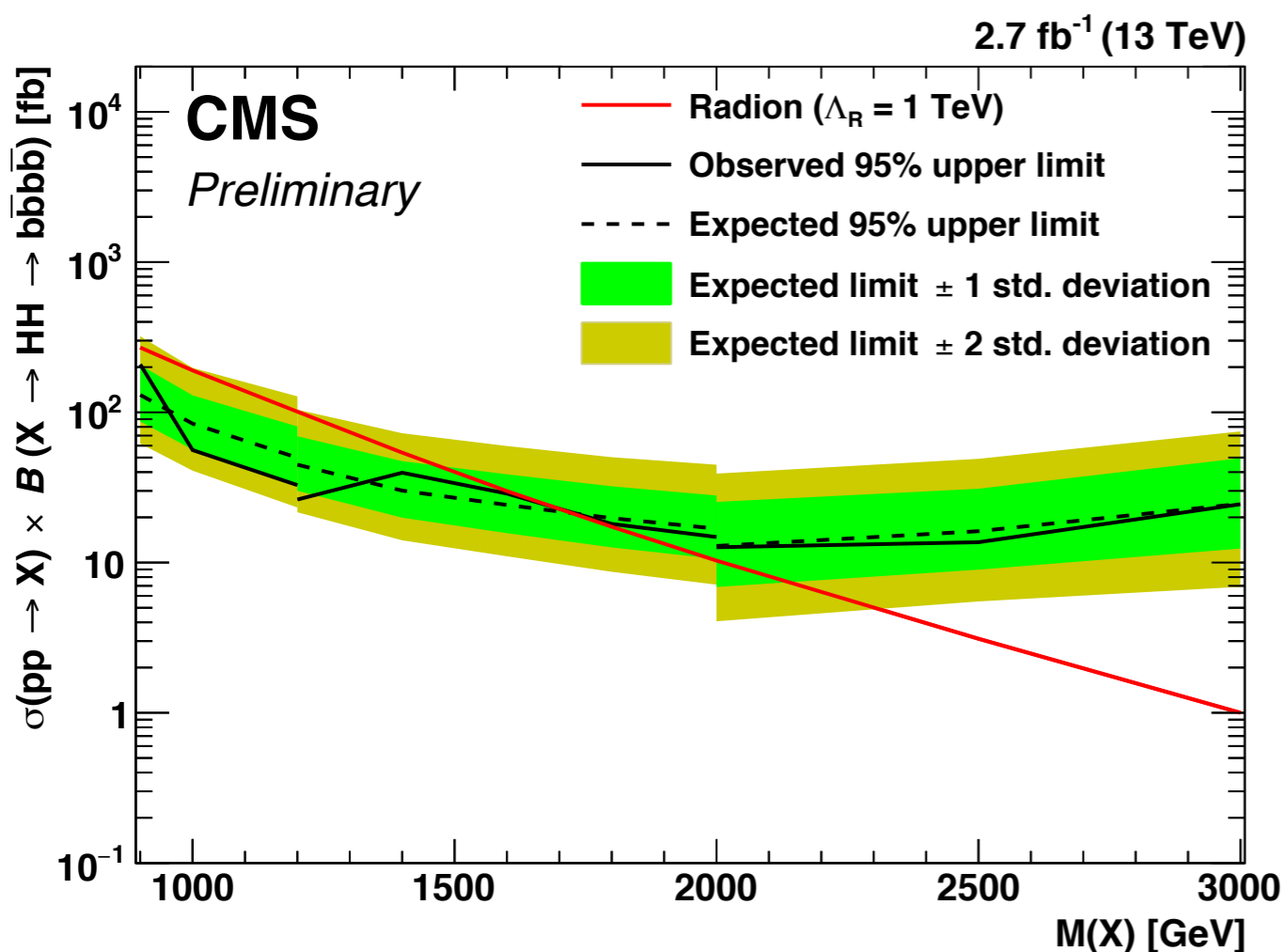


hh → bbbb: results

No evidence for the presence of new resonances so far over large mass range
 Sensitive to Radion (below 2TeV) and Graviton production (below 800GeV)

Boosted analysis:

- double b-tagger: at low/high mass
- sub-jets b-tagging: for $1200 < m_H < 2000$ GeV



hh → bbWW

Search for $hh \rightarrow bbWW \rightarrow bb2l2\nu$.

2 isolated OS leptons + 2 b-jets in the final state

2015 dataset at $\sqrt{s}=13$ TeV

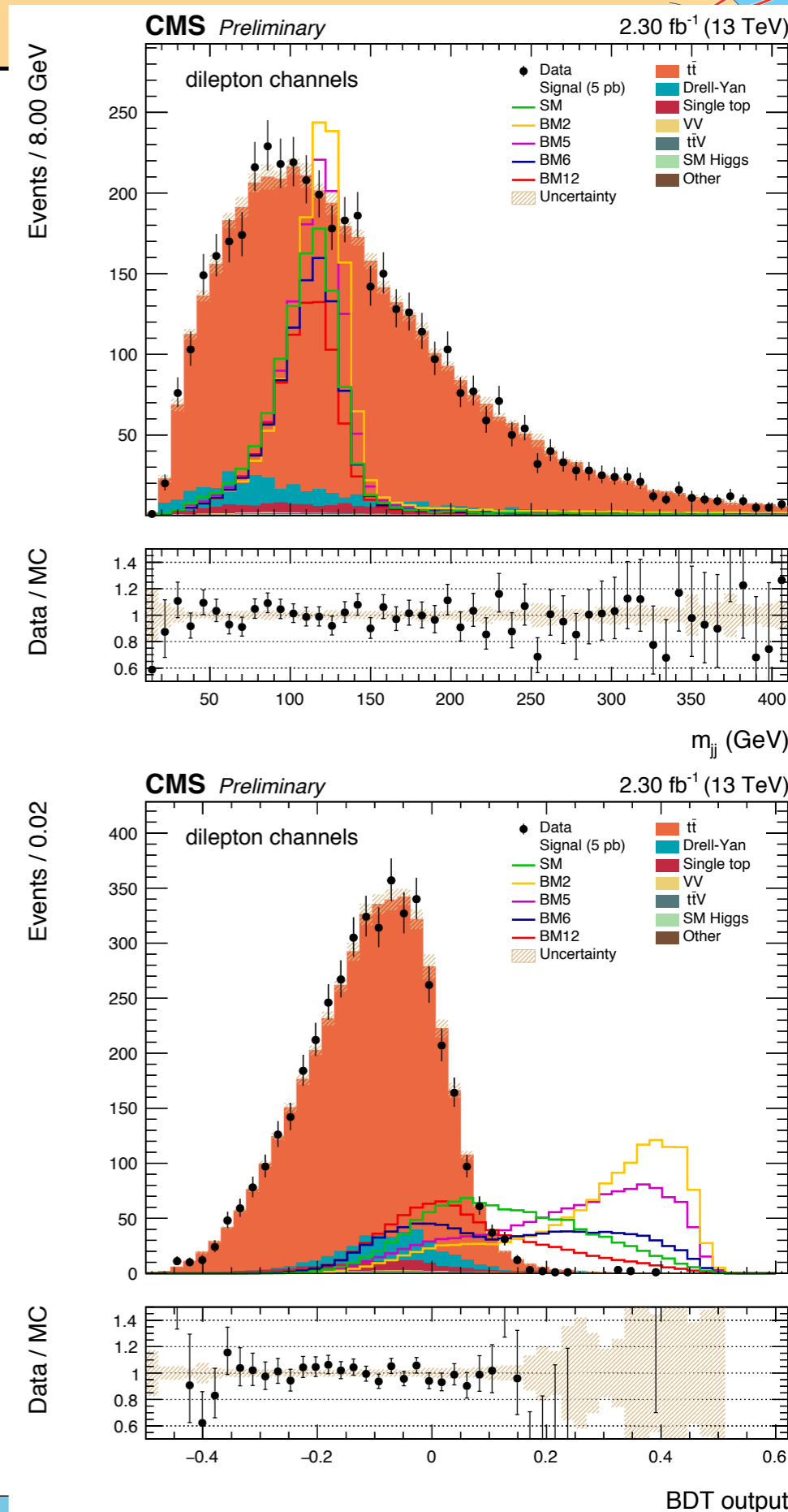
Final BR for $bb2l2\nu$ final state: 1.22%

Main backgrounds: $t\bar{t}$, DY, single top

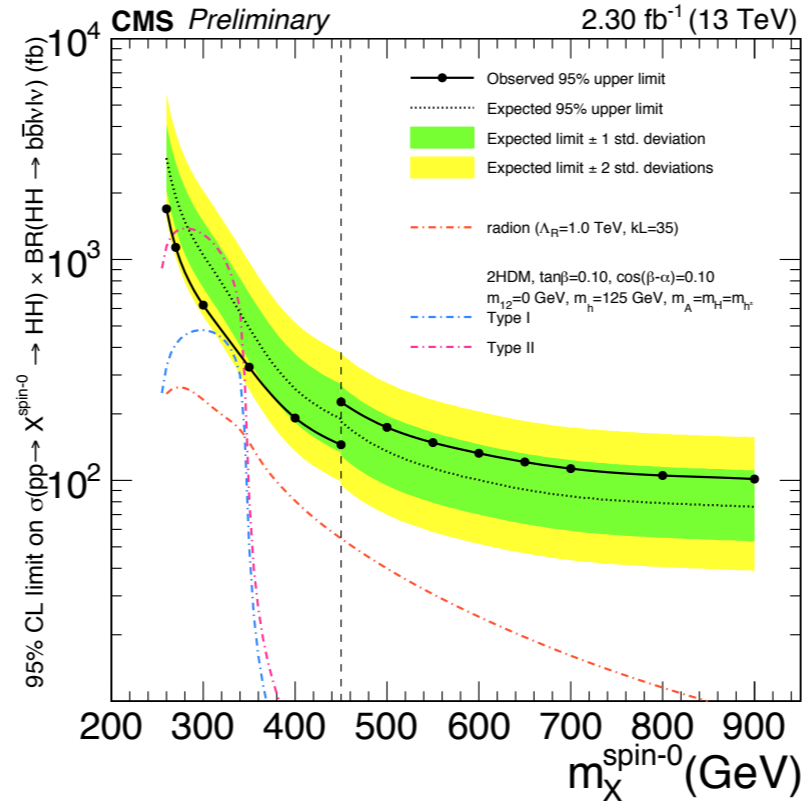
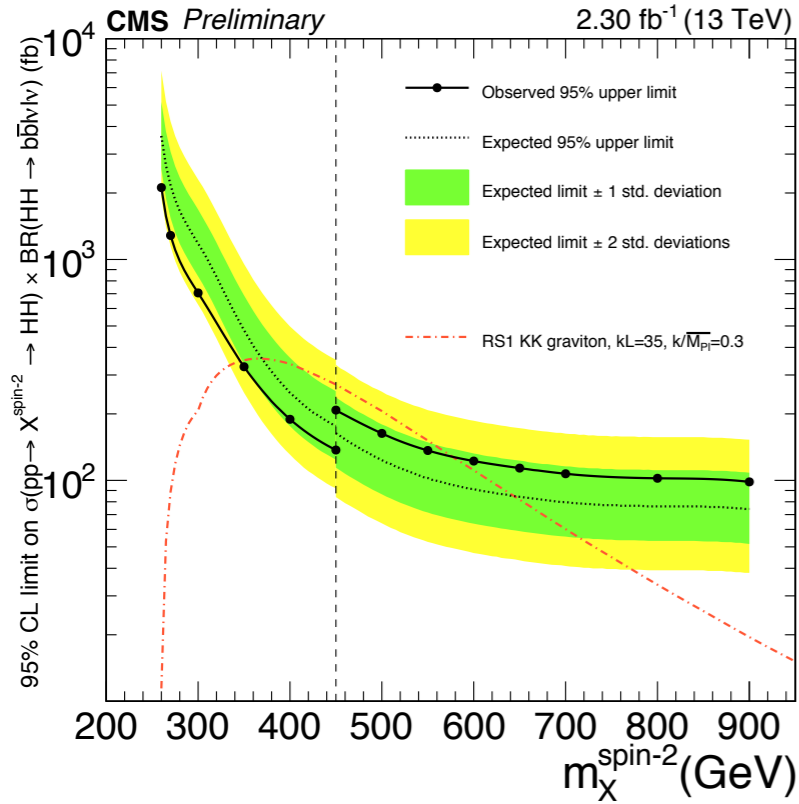
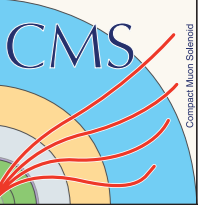
2 **BDT discriminants** (h masses, angles, transverse mass) to separate signal from background at low ($m_H < 450$) and high mass ($m_H > 450$). Optimised for $m_H = 400$ and $m_H = 650$. 1 **single BDT** trained for non-resonant searches.

Resonant: cut&count experiment in 4 categories: (m_{bb} -peak, m_{bb} -sidebands) x (low BDT, high BDT)

Non resonant: 2D fit in [$m(bb)$, BDT score] to extract the limits

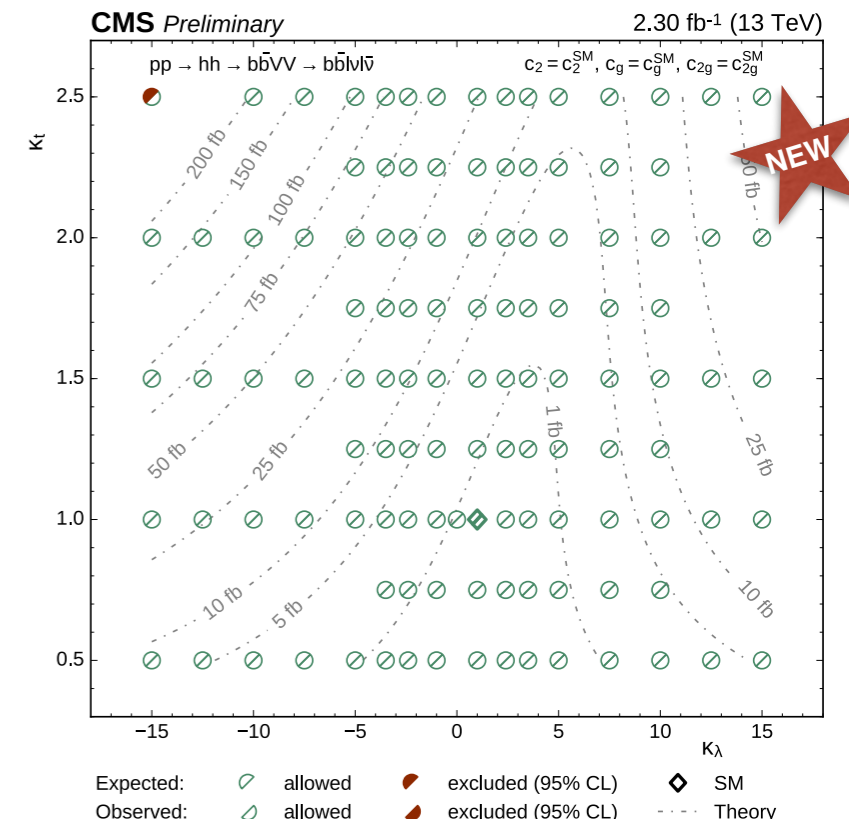
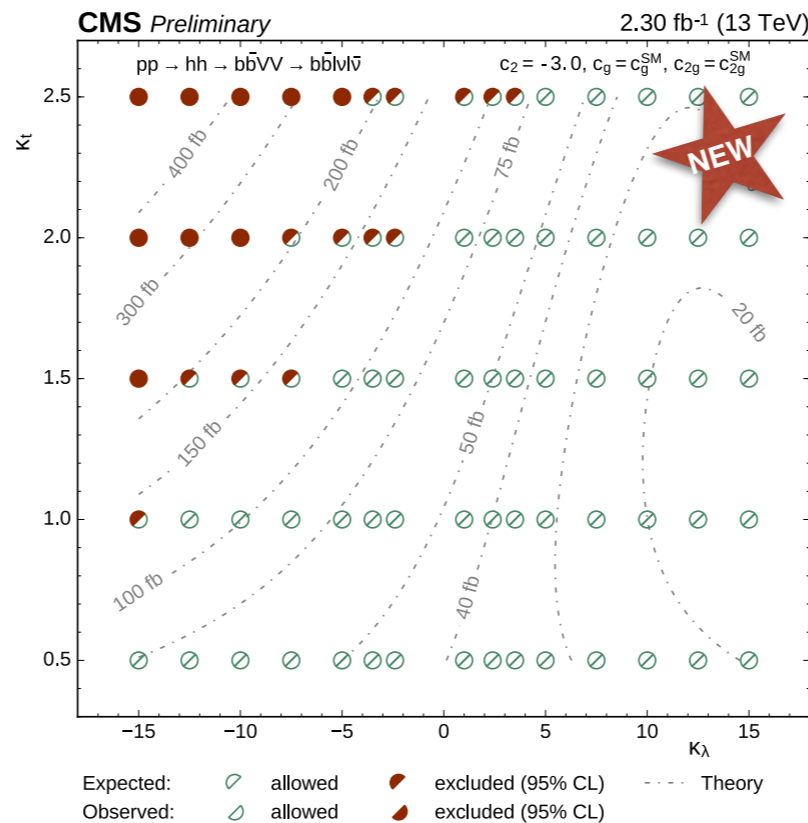
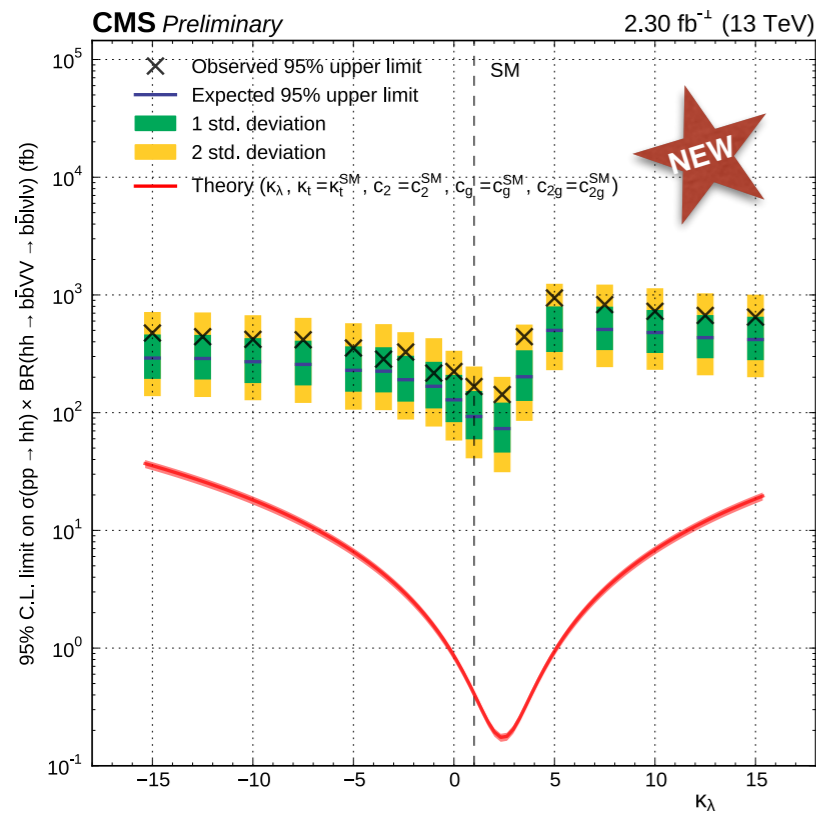


hh → bbWW: results

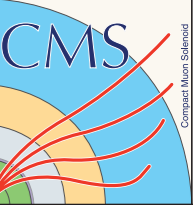


Spin-2 RSI KK-graviton excluded below 600 GeV

Non-resonant analysis sensitive to $O(400 \times \text{SM})$



hh → bbττ



Intermediate BR, fully reconstructed final state

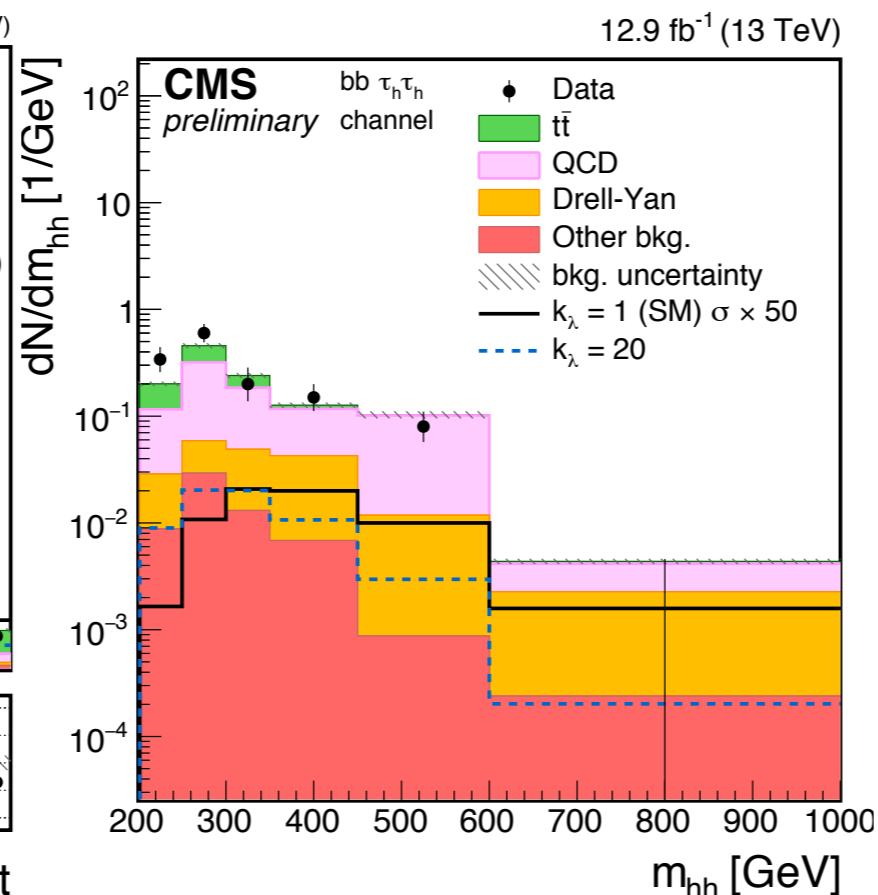
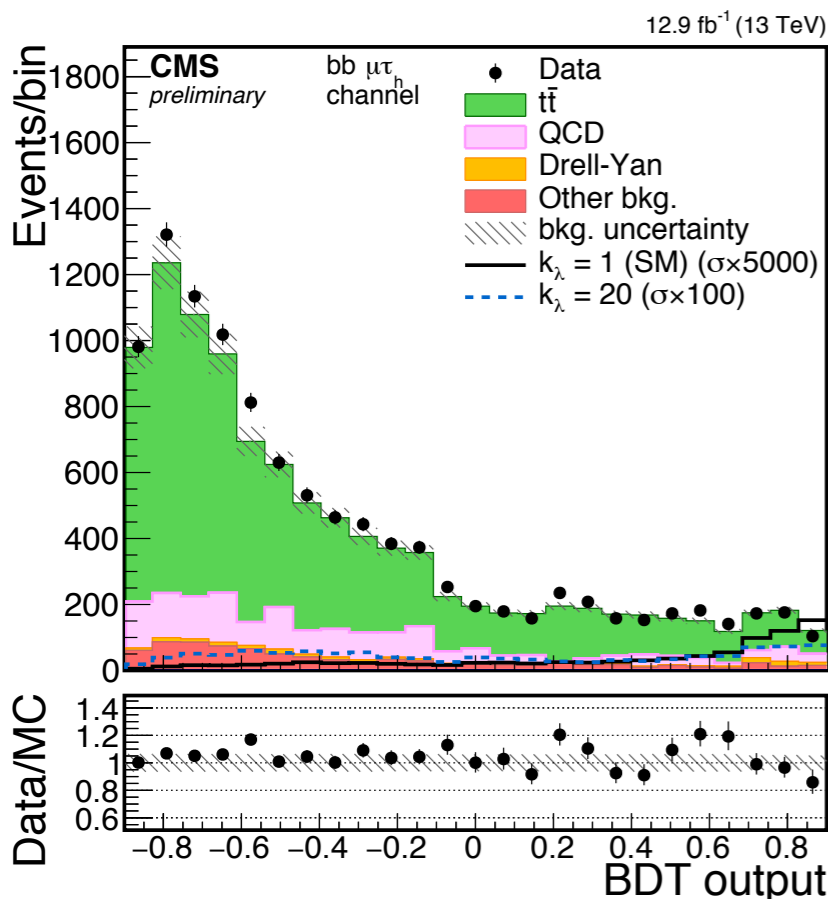
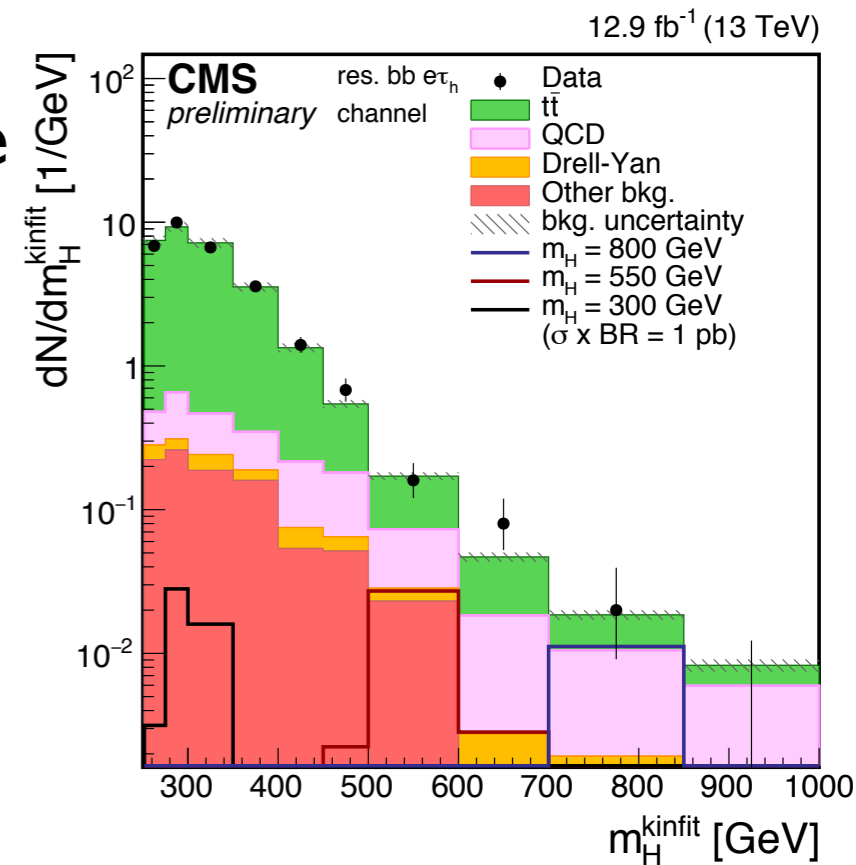
1 τ_H+1 isolated leptons (e, μ, τ_H)+2 b-jets in the final state

3 final states: eτ_H, μτ_H, τ_Hτ_H

Main bkg: tτ̄ (from MC), QCD multijet (from data in control regions)

Resonant search:

Limit extraction on kinematic fit of the 4-body invariant mass; 3 categories: 1bjet, 2bjet, boosted b-jets category



Non-resonant analysis:

- kinematic BDT discriminant to reduce tτ̄, only angular information
- visible mass as final variable

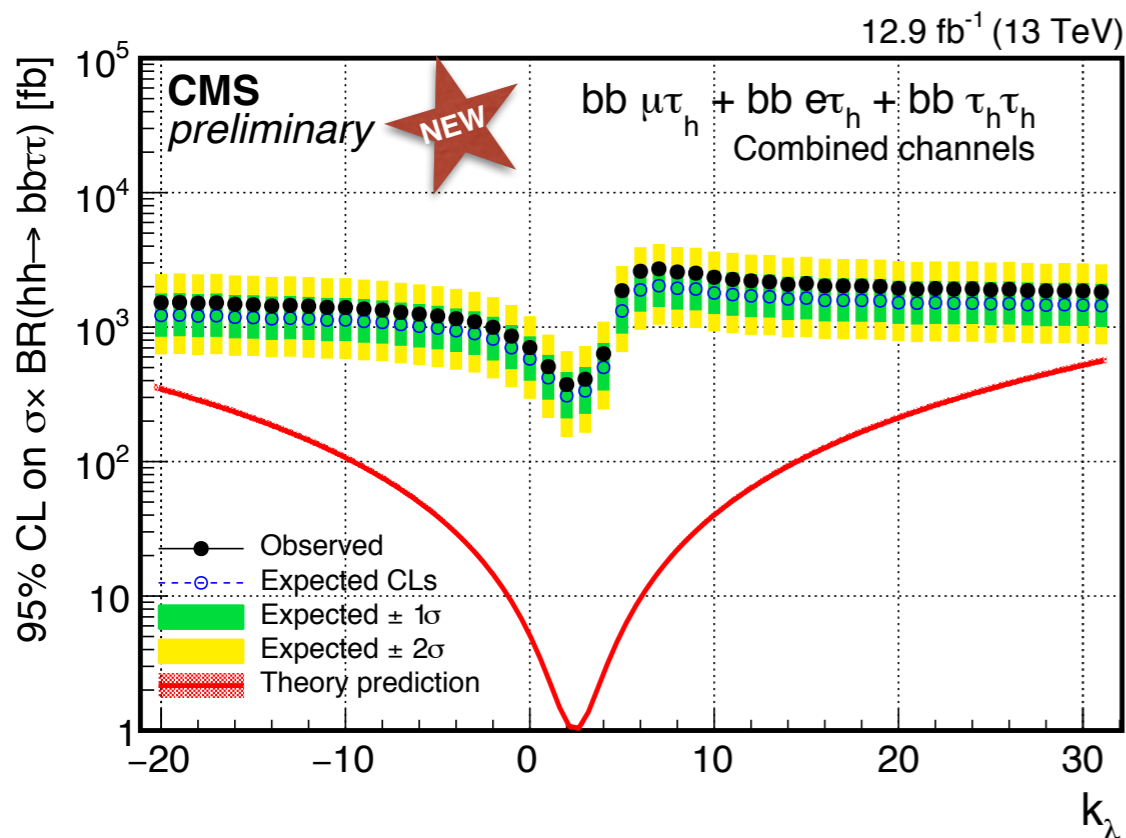
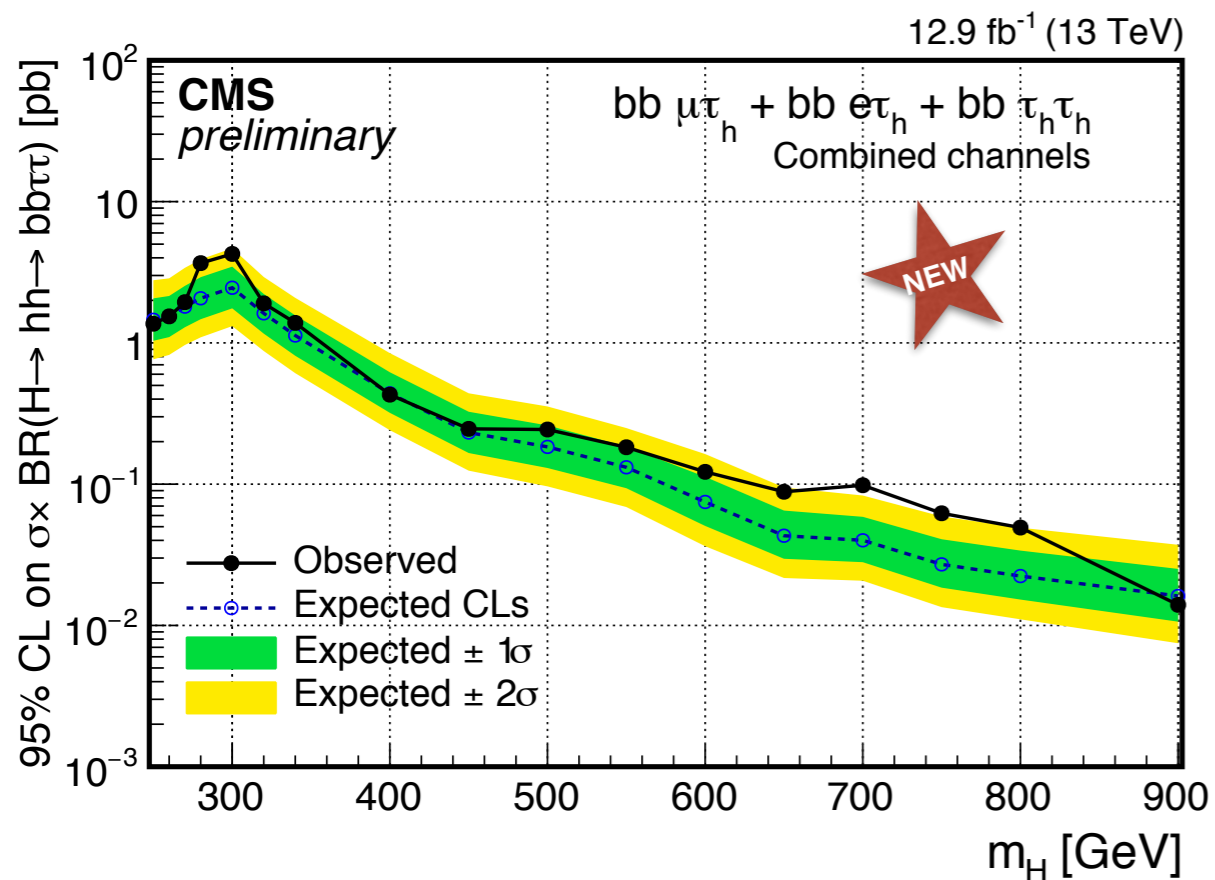
Only results on 2016 data shown.

Results with 2015 data:

CMS-PAS-HIG-012

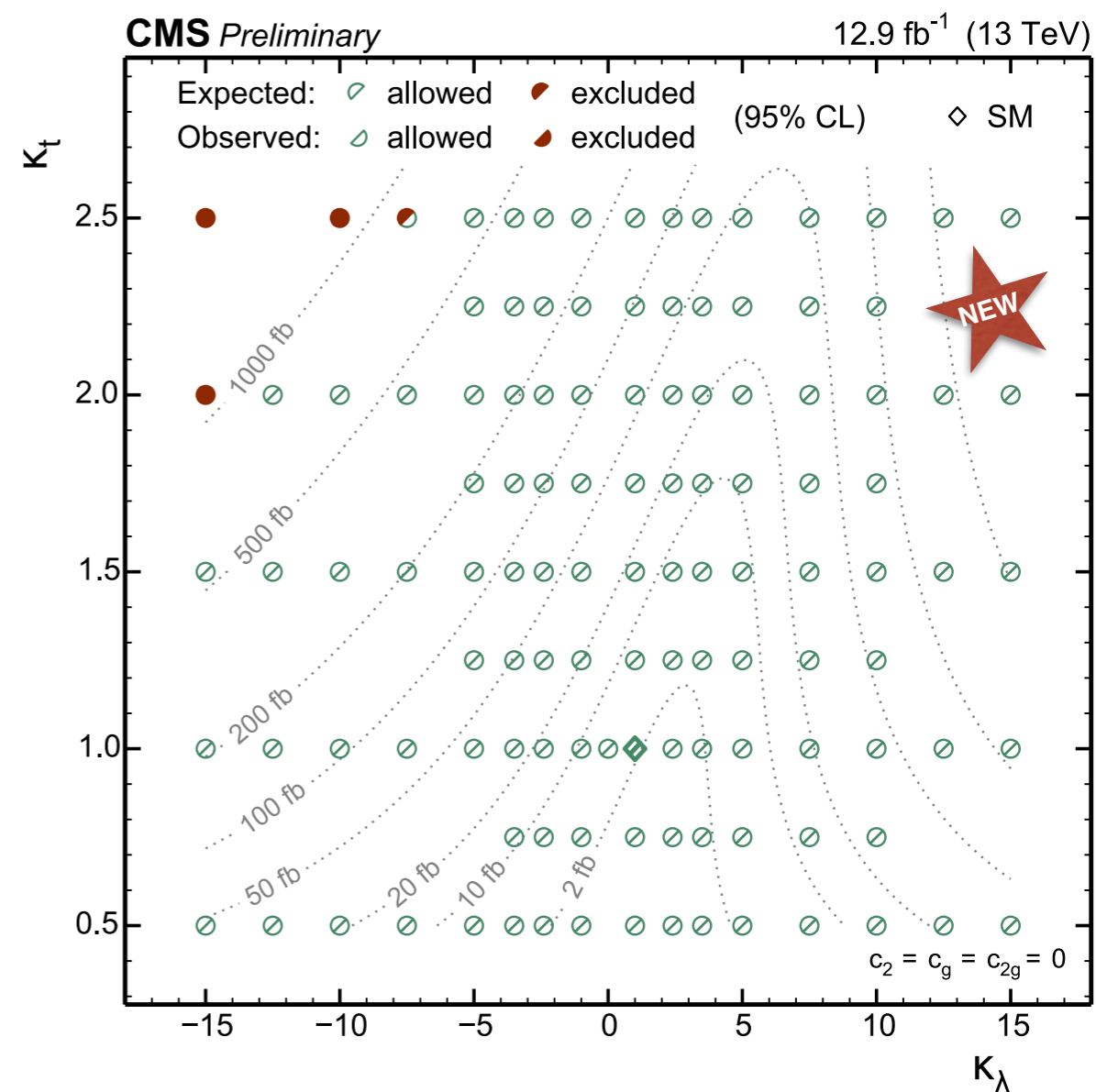
CMS-PAS-HIG-013

hh → bbττ: results



Non resonant limits starts to make dents in part of the 5D EFT model phase space

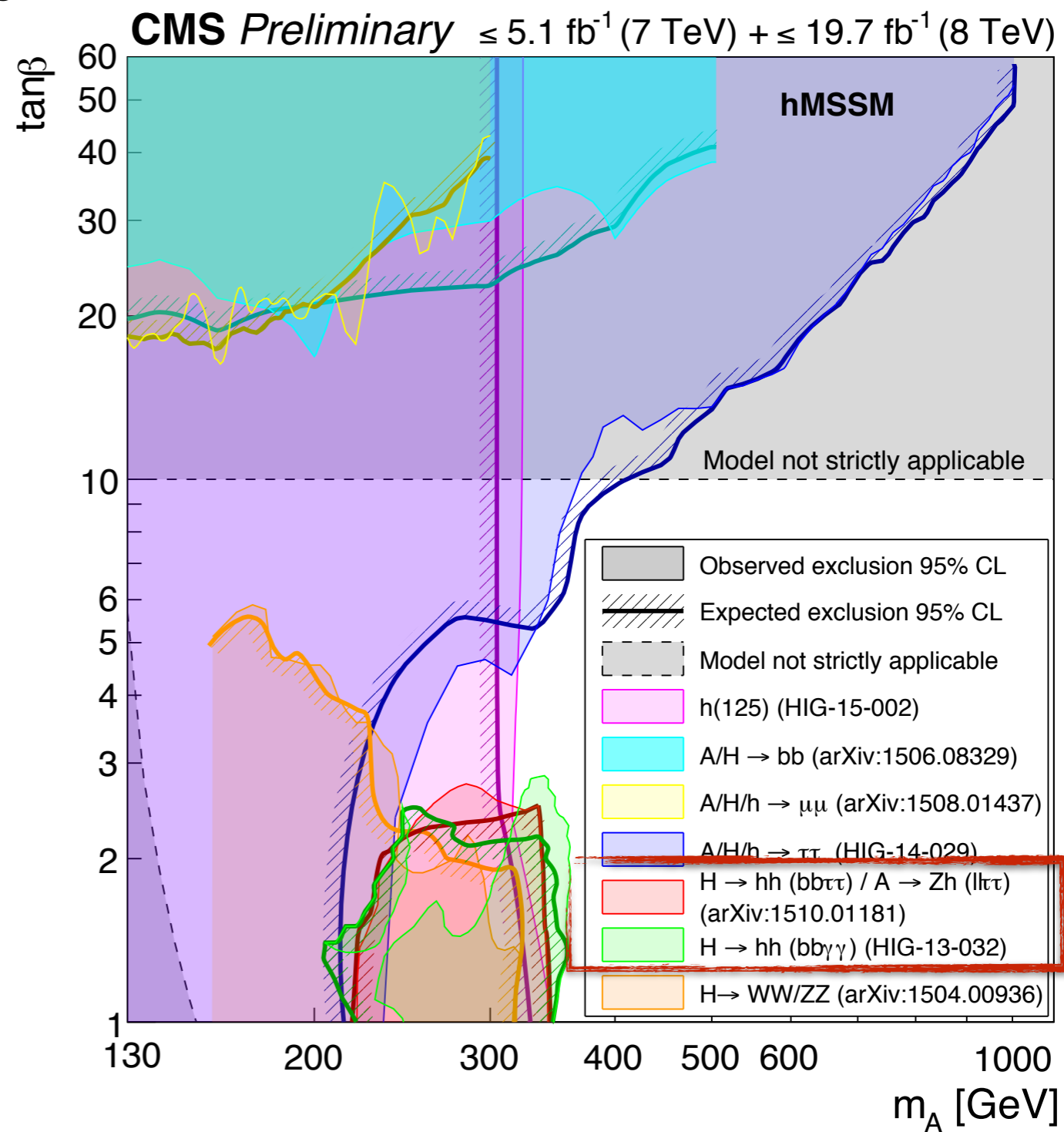
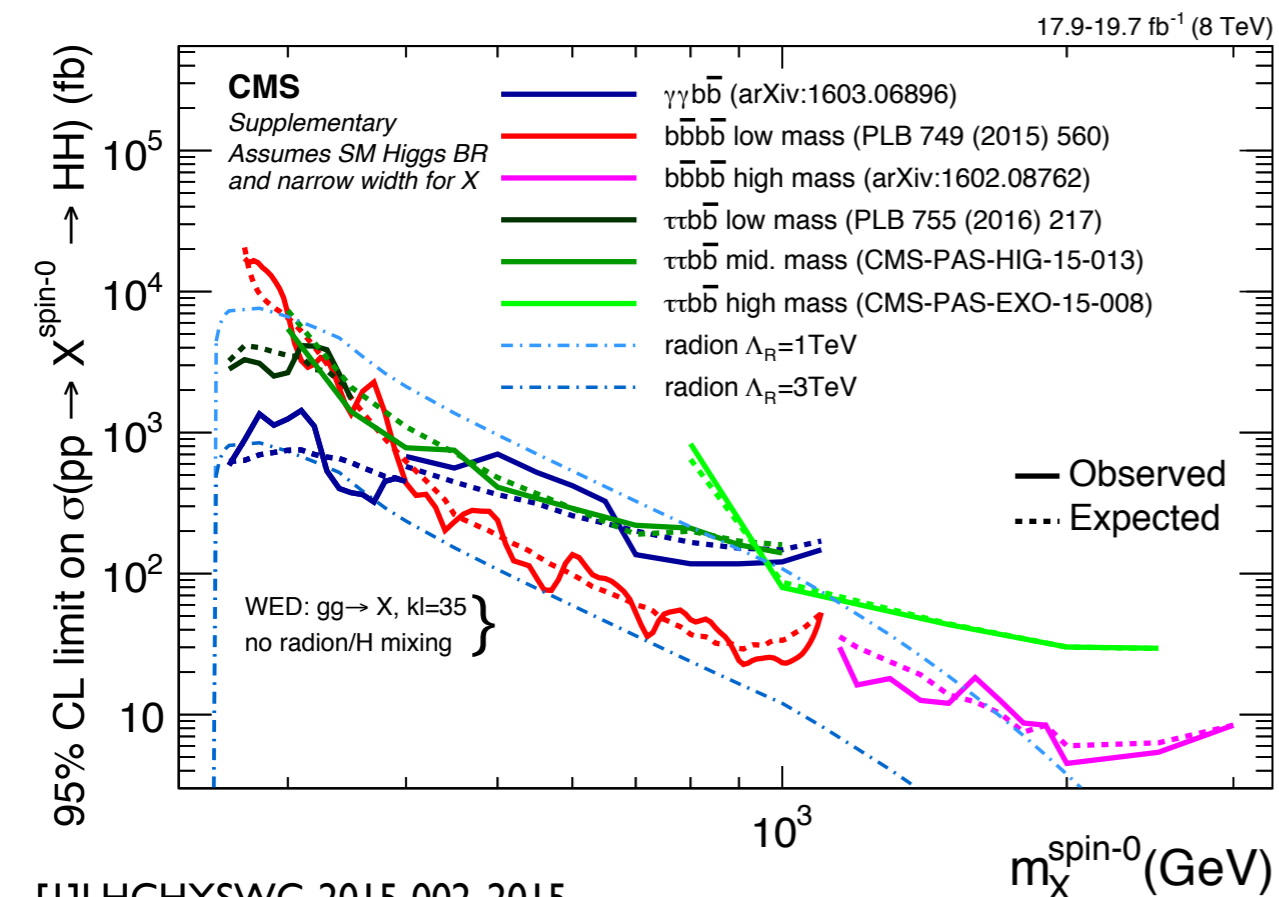
No significant excess observed in the resonant analysis



Summary of Run1 results



Several analysis performed at CMS
 Coverage ranges from $2m_h$ to few TeVs
 hMSSM: Effective MSSM model with $m_h = m_{H_0}$ ^[1]
 $H \rightarrow hh$ searches are providing an important coverage of the low m_A /low $\tan\beta$ region



Summary of Run2 results

$hh \rightarrow bbWW \rightarrow bb2l2\nu$: 2015 data

(2.3/fb) at $\sqrt{s}=13$ TeV

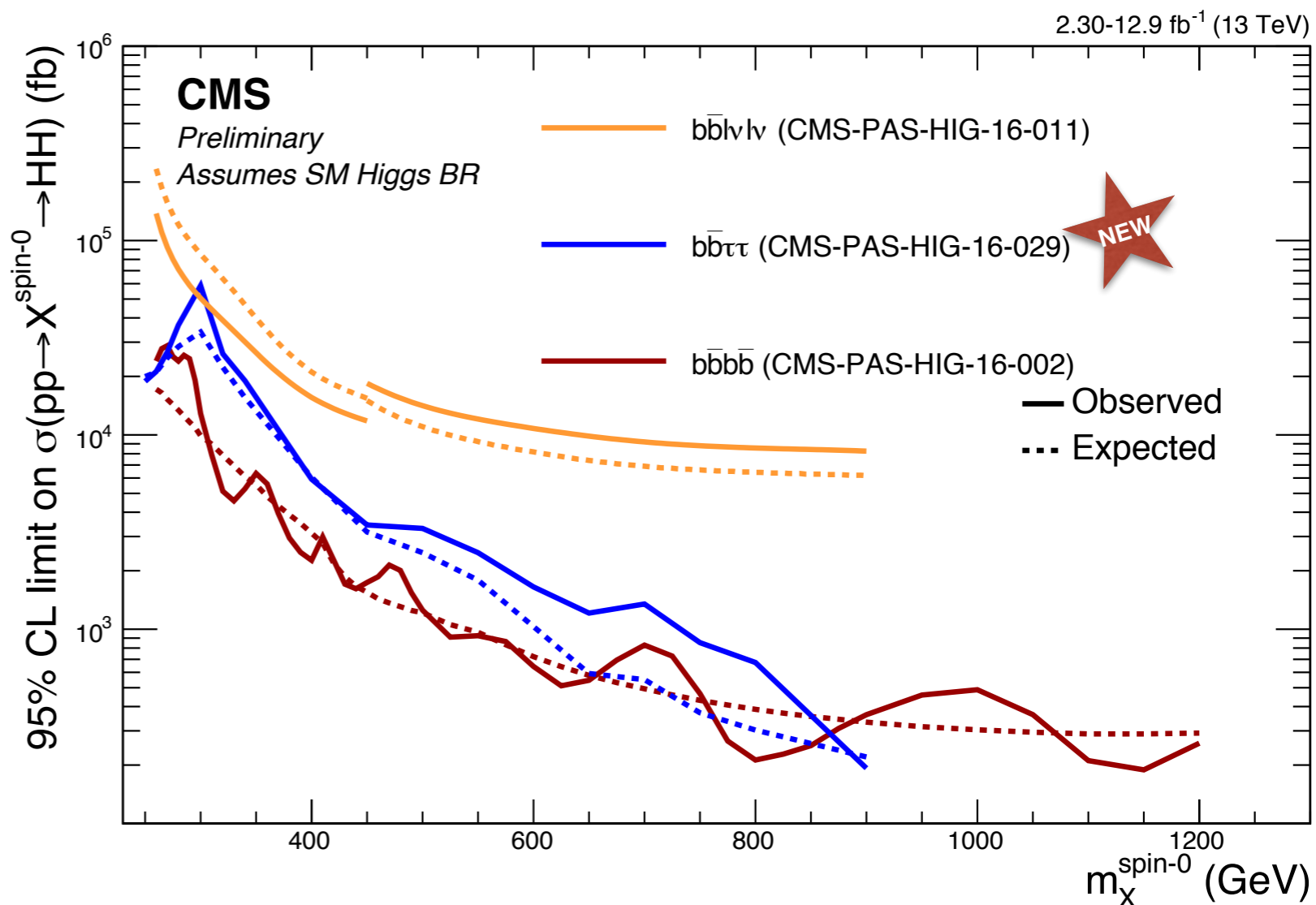
- 2 mass regions, optimised for $m_H=400$ and $m_H=650$

$hh \rightarrow bbbb$: 2015 data (2.3/fb) at $\sqrt{s}=13$ TeV

- Boosted regime not shown

$hh \rightarrow bb\tau\tau$: 2016 data (12.9/fb) at $\sqrt{s}=13$ TeV

- Boosted category to improve high mass sensitivity



Non-resonant production exclusion	
$bbWW$	410 \times $\sigma(\text{SM})$ ★ NEW
$bb\tau\tau$	200 \times $\sigma(\text{SM})$ ★ NEW
$bb\gamma\gamma$	74 \times $\sigma(\text{SM})$ (Run I)

Several competing analyses in **different final states** under study in CMS, providing excellent coverage in different decay modes.

Non resonant double Higgs production is the main way to measure Higgs self-coupling.

- At the moment, we can probe $O(10-100 \times SM)$. Much larger luminosity is needed to reach SM sensitivity, but we are starting to probe BSM and to constraint exotic BSM

Resonant searches can already provide important constrain on BSM physics (MSSM, WED, heavy scalars).

- KK-graviton excluded below 800 GeV, $\Lambda_R = 1$ TeV Radion below 2 TeV

Further improvement awaited with end-of-the-year luminosity and the **combination of the results** among all channels

Exciting prospects for double Higgs searches

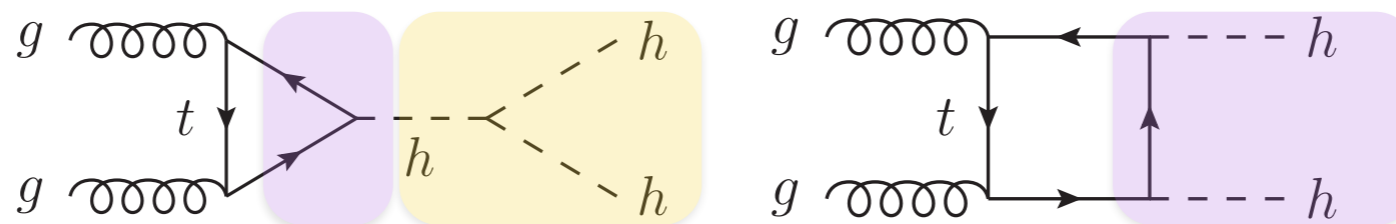
BACKUP

gg → hh parametrization

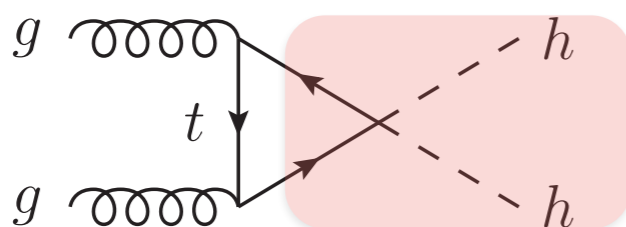
The relevant lagrangian terms of gg → HH production in D=6 EFT

$$\mathcal{L}_{hh} = - \frac{m_h^2}{2v} \left(1 - \frac{3}{2}c_H + c_6 \right) h^3 + \frac{\alpha_s c_g}{4\pi} \left(\frac{h}{v} + \frac{h^2}{2v^2} \right) G_{\mu\nu}^a G_a^{\mu\nu} - \left[\frac{m_t}{v} \left(1 - \frac{c_H}{2} + c_t \right) \bar{t}_L t_R h + \text{h.c.} \right] - \left[\frac{m_t}{v^2} \left(\frac{3c_t}{2} - \frac{c_H}{2} \right) \bar{t}_L t_R h^2 + \text{h.c.} \right]$$

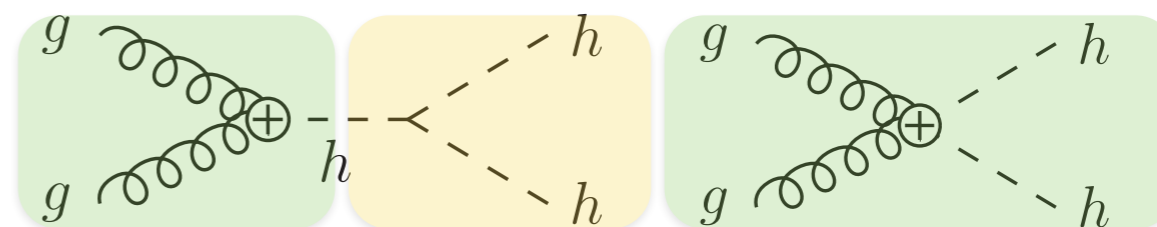
arXiv:1410.3471



SM diagrams



ttHH non-linear interaction



Higgs-gluon contact interactions

An EFT implementation for hh

The double Higgs production cross section can be written as a function of the 5 EFT parameters: λ_{hhh} , y_t , c_2 , c_{2g} , c_g

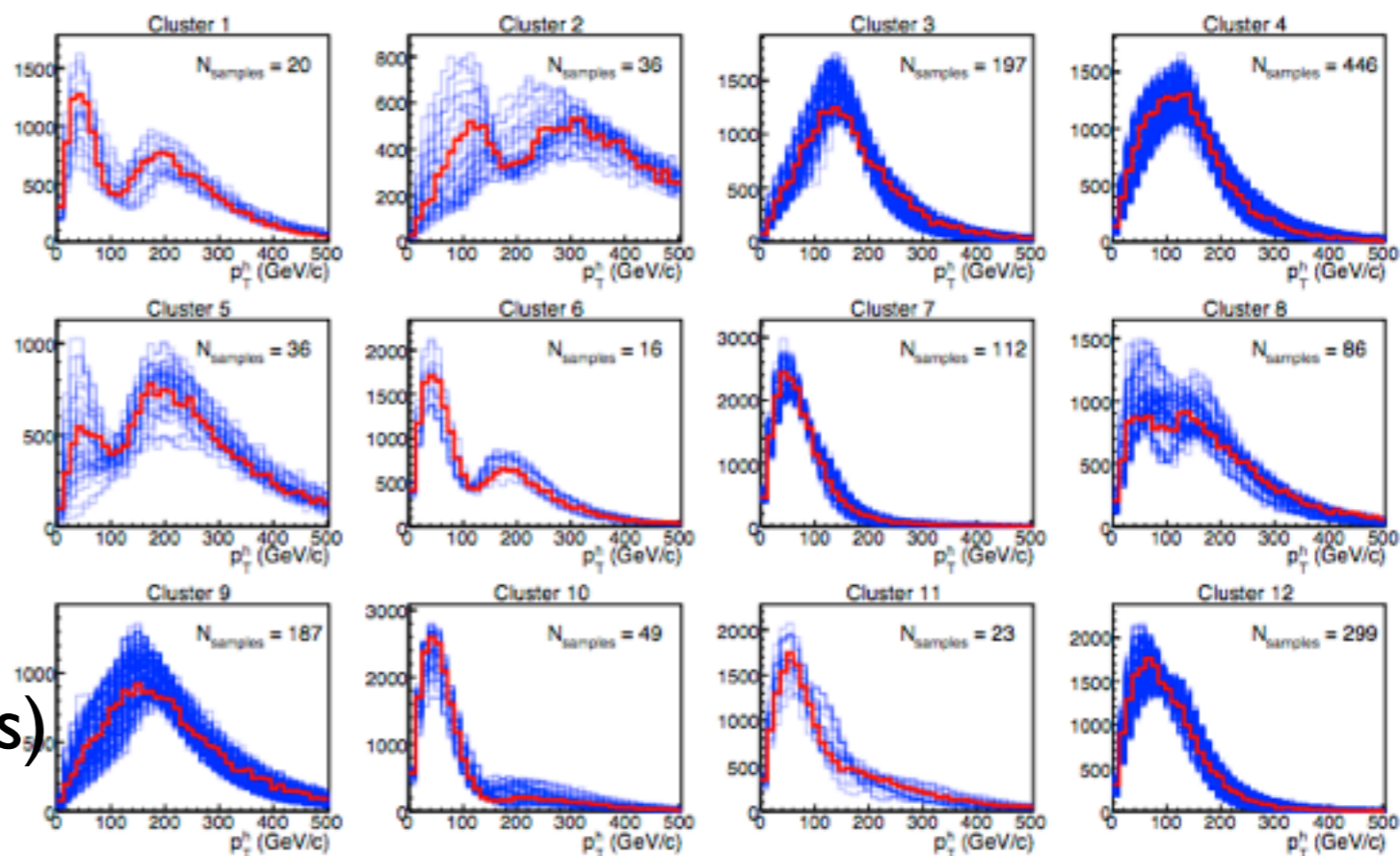
$$R_{hh} \equiv \frac{\sigma_{hh}}{\sigma_{hh}^{SM}} \stackrel{LO}{=} A_1 \kappa_t^4 + A_2 c_2^2 + (A_3 \kappa_t^2 + A_4 c_g^2) \kappa_\lambda^2 + A_5 c_{2g}^2 + (A_6 c_2 + A_7 \kappa_t \kappa_\lambda) \kappa_t^2 + (A_8 \kappa_t \kappa_\lambda + A_9 c_g \kappa_\lambda) c_2 + A_{10} c_2 c_{2g} + (A_{11} c_g \kappa_\lambda + A_{12} c_{2g}) \kappa_t^2 + (A_{13} \kappa_\lambda c_g + A_{14} c_{2g}) \kappa_t \kappa_\lambda + A_{15} c_g c_{2g} \kappa_\lambda.$$

JHEP 04 (2016) 126

2D ($M_{HH}, \cos\vartheta^*$) signal shapes from different points in the 5D EFT phase space are clustered together.

12 clusters are identified according to their kinematical properties

Inside each cluster, a representative shape is identified, as the one with the minimum distance (in the test statistics) from all other shapes in the cluster



Each point of the phase space can be mapped by means of its cross-section and representative shape

hh → bbγγ

Lowest BR of all channels considered, but excellent resolution on $m_{\gamma\gamma}$

Selection: $p_{T\gamma^1}/m_{\gamma\gamma} < 1/3$, $p_{T\gamma^2}/m_{\gamma\gamma} < 1/4$ + mass cuts

Two categories: 1 b-jet (low purity category), ≥ 2 b-tagged jets (high purity)

Different signal regions at low and high mass

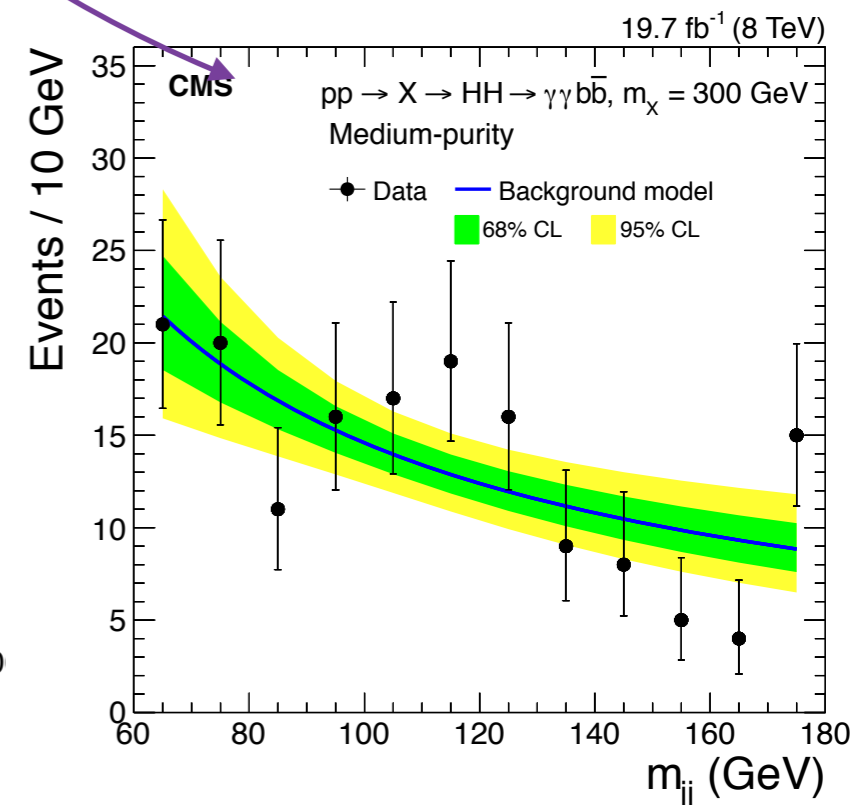
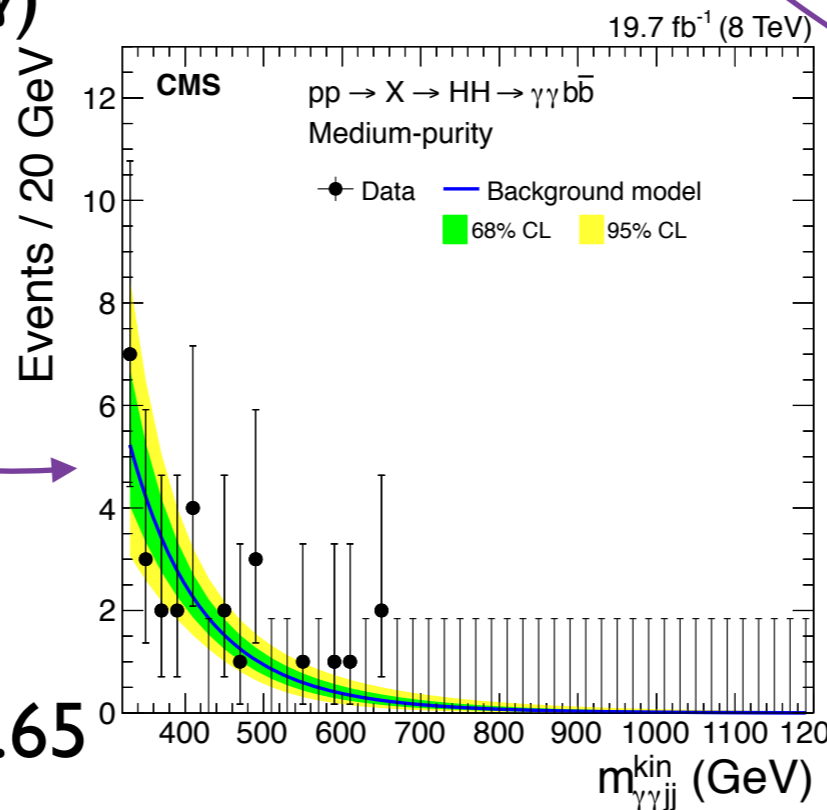
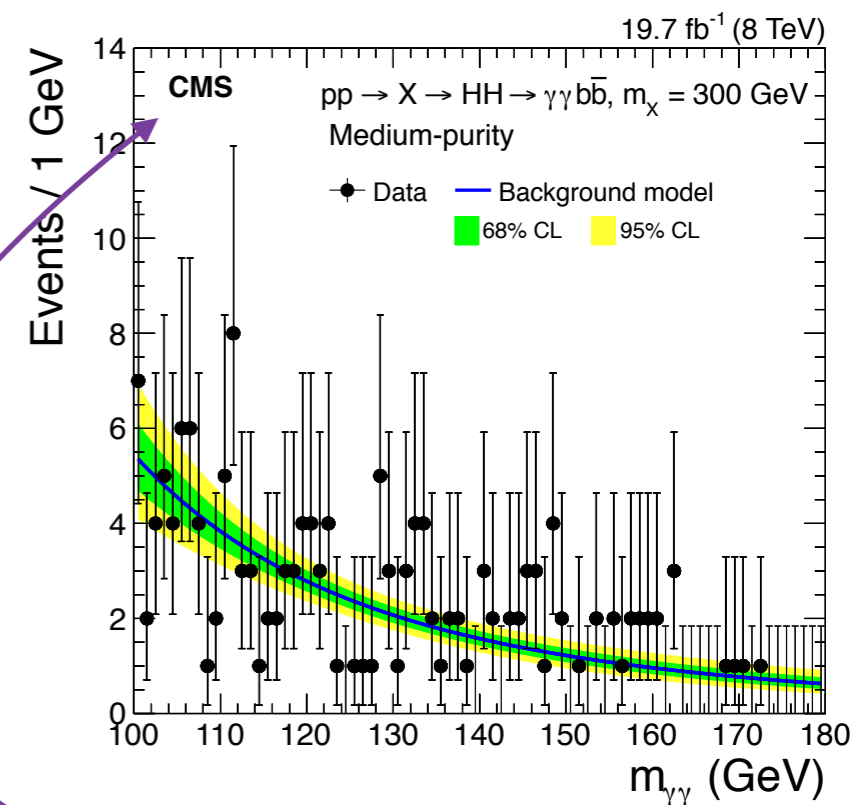
- $m_H < 400$ GeV: **b-jet regression** + **2D signal fit** extraction based on $(m_{jj}, m_{\gamma\gamma})$

- $400 < m_H < 1100$ GeV: **kinematic fit** of the 4-body invariant mass

Non-resonant analysis:

2 b-tag cat. X 2 cat. $m_{\gamma\gamma}$

- $m_{\gamma\gamma} < 350$ && $|\cos\theta^{CS}| < 0.65$
- $m_{\gamma\gamma} > 350$ && $|\cos\theta^{CS}| < 0.9$



hh → bbγγ

Lowest BR of all channels considered, but excellent resolution on $m_{\gamma\gamma}$

Selection: $p_T^{\gamma^1}/m_{\gamma\gamma} < 1/3$, $p_T^{\gamma^2}/m_{\gamma\gamma} < 1/4$ + mass cuts

Two categories: 1 b-jet (low purity category), ≥ 2 b-tagged jets (high purity)

Different signal regions at low and high mass

- $m_H < 400$ GeV: **b-jet regression** + **2D signal fit** extraction based on $(m_{jj}, m_{\gamma\gamma})$

- $400 < m_H < 1100$ GeV: **kinematic fit** of the 4-body invariant mass

Non-resonant analysis:

2 b-tag cat. X 2 cat. $m_{\gamma\gamma}$

- $m_{\gamma\gamma} < 350$ && $|\cos\vartheta^{CS}| < 0.65$
- $m_{\gamma\gamma} > 350$ && $|\cos\vartheta^{CS}| < 0.9$

Signal hypothesis	Select	# categories	Fit
(1) $m_X \leq 400$ GeV	$m_{\gamma\gamma jj}^{\text{kin}}$	2 (b tags)	$m_{\gamma\gamma}, m_{jj}$
(2) $m_X \geq 400$ GeV	$m_{\gamma\gamma}, m_{jj}$	2 (b tags)	$m_{\gamma\gamma}^{\text{kin}}$
(3) Nonresonant	$ \cos\theta_{HH}^{\text{CS}} $	4 (b tags, $m_{\gamma\gamma}^{\text{kin}}$)	$m_{\gamma\gamma}, m_{jj}$

Photons		Jets	
Variable	Range	Variable	Range
$p_T^{\gamma^1}/m_{\gamma\gamma}$	$> 1/3$	p_T^j (GeV)	> 25
$p_T^{\gamma^2}/m_{\gamma\gamma}$	$> 1/4$		
$ \eta_\gamma $	< 2.5	$ \eta_j $	< 2.4
$m_{\gamma\gamma}$ (GeV)	[100, 180]	m_{jj} (GeV)	[60, 180]
		b-tagged jets	> 0